A NUMERICAL TWO-TIME APPROACH FOR RF-IC ANALYSIS

Mihai IORDACHE, Lucia DUMITRIU, Grigore STAMATESCU

"Politehnica" University of Bucharest, Electrical Engineering Department,
Spl. Independentei 313, Cod 06 0042, Bucharest ROMANIA,
Phone/Fax (+4021) 318 10 16 iordache@elth.pub.ro

***Abstract* – The paper presents a new version of state variable method for circuit analysis with widely separated time scales. Widely-separated time scales appear in many electronic circuits, making traditional analysis difficult even impossible if the circuits are highly nonlinear. The key idea is to use multiple time variables, which enable signals with widely separated rates of variation to be represented efficiently. The differential algebraic equations (DAEs) describing the RF-IC circuits are transformed in multi-time partial differential equations (MPDEs). Using the new numerical technique results in computation time and memory significant gain. In order to solve MPDE we use the associated resistive discrete equivalent circuits (companion circuits) for the dynamic circuit elements.**

Keywords: *Multiple time variables, Radio frequency analog circuit analysis.*

1. INTRODUCTION

A very important step in radio-frequency integrated circuits (RF-IC) design is the circuit simulation. The RF-IC applications has carrier frequencies in the GHz-range with modulating signals in the kHz-range. Due to the broad signal spectrum (about six orders of magnitude) finding of the steady-state by the *brute-force method* is very time consuming [1, 2]. These signals are called *multirate signals*, and they contain "components" that vary at two or more widely separated rates. Such signals arise in various physical systems, as communication circuits (up/down-converters, automatic gain-control circuits), cycle-chopping and switched power converters, switched-capacitor filters, pulsewidth-modulation circuits etc. These systems are typically difficult to analyze using traditional numerical integration algorithms, such as those used in programs like SPICE [1]. The difficulty consists in the widely disparate rates: following fast-varying signal components long enough to obtain information about the slowly-varying ones is computationally expensive, and can also be inaccurate.

Many multirate signals can be represented efficiently as functions of two or more time variables, i.e. as *multivariate functions*. If a circuit is described with differential-algebraic equations (DAE), using multivariate functions for the unknowns leads naturally to a partial differential equation (PDE) form called *Multirate Partial Differential Equation* (*MPDE*). If we apply time-domain numerical methods to solve the MPDE directly for the multivariate forms of the unknowns, we are able to analyze the combination of strong nonlinearities and multirate signals.

In the case of the lumped analog nonlinear circuits, because the numerical differentiation is a relatively inaccurate operation, we approximate the $q_k - v_k$ characteristic of each nonlinear capacitor and the $\varphi_k - i_k$ characteristic of each nonlinear inductor by piecewise-linear segments. In order to simplify the description of the nonlinear resistors, their $v - i$ characteristics may be approximated by piecewise-linear continuous curves, or by new characteristics in which the nonlinearities are transferred to the sources, [8 - 12]. Using the state equations (SEs) in partially symbolic form, we obtain a significant efficiency in circuit design and an improvement of the accuracy in the numerical calculations by considering as symbols only the parameters corresponding to the nonlinear circuit elements.

SEs for lumped piecewise-linear nonlinear analogue circuits have the following form [11-13]:

$$\dot{\boldsymbol{x}} = \boldsymbol{A}\boldsymbol{x} + \boldsymbol{B}\boldsymbol{y} + \boldsymbol{B}_1\dot{\boldsymbol{y}} \qquad (1)$$

where: the matrices $\boldsymbol{A}$, $\boldsymbol{B}$ and $\boldsymbol{B}_1$ contain the incremental capacitances, the incremental inductances, the incremental resistances and the incremental conductances corresponding to the nonlinear circuit elements, $\boldsymbol{x}(t) = \left[\boldsymbol{v}_{Ct}^{\mathrm{t}}, \boldsymbol{i}_{Lc}^{\mathrm{t}}\right]^{\mathrm{t}}$ - is the state variable vector (v_{Ct} - the tree branch capacitor voltages and i_{Lc} - the link inductor currents) with $\boldsymbol{x}_0 = \boldsymbol{x}(t_0)$ initial condition; $\boldsymbol{y} = \left[\boldsymbol{e}^{\mathrm{t}}, \boldsymbol{j}^{\mathrm{t}}\right]^{\mathrm{t}}$ - is the input vector, and the superscript "t" denotes the transpose. If the analyzed circuit exhibits multirate behaviour, its variables can be represented efficiently using multiple time variables. If there are *p* multivariate forms of change, *p* time-scales are used. We denote the multivariate forms of $\boldsymbol{x}(t)$ and $\boldsymbol{y}(t)$ by $\hat{\boldsymbol{x}}(t_1,...,t_p)$ and $\hat{\boldsymbol{y}}(t_1,...,t_p)$.

The MPDE corresponding to (1) is:

$$\frac{\partial \hat{\boldsymbol{x}}}{\partial t_1}+...+\frac{\partial \hat{\boldsymbol{x}}}{\partial t_p}=\boldsymbol{A}\hat{\boldsymbol{x}}+\boldsymbol{B}\hat{\boldsymbol{y}}+\boldsymbol{B}_1\left(\frac{\partial \hat{\boldsymbol{y}}}{\partial t_1}+...+\frac{\partial \hat{\boldsymbol{y}}}{\partial t_p}\right) \quad (2)$$

In [1] it is shown that there is a relation between the MPDE and the SEs of the circuit. According to the theorem 1 from [1] the solutions of the SEs are available on the "diagonal" lines along the MPDE multivariate solutions.

Because the SEs are easy to implement in a program, we use these equations to obtain numerical solution of the MPDE. Replacing each capacitor and each inductor (magnetic coupled or not) by a discrete resistive circuit model associated with an implicit numerical integration algorithm, the transient analysis of the nonlinear circuits can be reduced to the dc analysis of a sequence of equivalent nonlinear resistive circuits [4-7, 11, 12]. By using the backward differential formula of high order, the efficiency is achieved without compromising accuracy.

2. DESCRIPTION OF THE METHOD

Considering the two-rate case, MPDE (2) becomes:

$$\frac{\partial \hat{\boldsymbol{x}}}{\partial t_1}+\frac{\partial \hat{\boldsymbol{x}}}{\partial t_2}=\boldsymbol{A}\hat{\boldsymbol{x}}+\boldsymbol{B}\hat{\boldsymbol{y}}+\boldsymbol{B}_1\left(\frac{\partial \hat{\boldsymbol{y}}}{\partial t_1}+\frac{\partial \hat{\boldsymbol{y}}}{\partial t_2}\right) \quad (3)$$

with the periodic boundary conditions (BCs) $\hat{\boldsymbol{x}}(t_1+T_1,t_2+T_2)=\hat{\boldsymbol{x}}(t_1,t_2)$. We consider a uniform grid $\{\bar{t}(i,j)\}$ of size $(n_1+1)\times(p_2+1)$ on the rectangle $[0,m_1T_1]\times[0,T_2]$ (Fig.1), where $\bar{t}(i,j)=(t_{1\_i},t_{2\_j})$, with $t_{1-i}=(i-1)h_1$, $t_{2\_j}=(j\text{-}2)T_2+(j\text{-}1)h_2$, $i=\overline{1,n_1+1}$, $j=\overline{1,p_2+1}$; $h_1=m_1T_1/n_1 = T_1/p_1$, and $h_2=T_2/p_2$. Consider that the slow components of $\boldsymbol{b}(t)$ and $\boldsymbol{x}(t)$ depend on t_1 and the fast components depend on t_2.

In order to integrate the state equation (1) we use the *backward-differentiation formula* (BDF) which approximates to within prescribed accuracy the present value $\dot{x}(t_{n+1})$ of the time derivative of $x(t_{n+1})$ in terms of x_{n+1} and p past values $x_n, x_{n-1},...,x_{n-p+1}$:

$$\dot{x}_{n+1}=\frac{1}{h}\sum_{k=0}^{p}a_k x_{n+1-k}=\frac{1}{h}\left(x_{\_n}-x_{\_o}\right) \quad (4)$$

where: $a_0,a_1,...,a_p$ are constants, $h=t_{n+1}-t_n$ is the present step size, $x_{\_n}=a_0x_{n+1}$ is the new value of x, and $x_{\_o}$ is the "old" value.

We can also use other numerical implicit integration algorithms like the trapezoidal algorithm or one of Gear's algorithms.

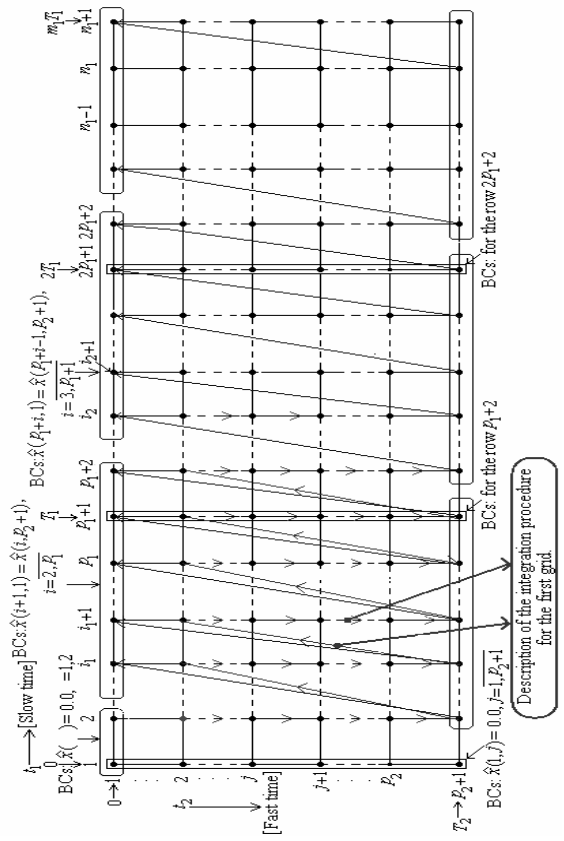

Figure 1. A uniform grid $\{\bar{t}(i,j)\}$ of size $(n_1+1)\times(p_2+1)$.

For the first periods T_1 and T_2 (corresponding to the grid of size $(p_1+1)\times(p_2+1)$), we assume that the BCs are $\hat{\boldsymbol{x}}(1,j)=0.0$, $j=\overline{1,p_2+1}$ and $\hat{\boldsymbol{x}}(i,1)=0.0$, i =1,2; $\hat{\boldsymbol{x}}(i+1,1)=\hat{\boldsymbol{x}}(i,p_2+1)$, $i=\overline{2,p_1}$; on the row $t_1=0$, and on the column $t_2=0$ respectively. We start the integration process on the row 2 from the point $\bar{t}(2,2)=(t_{1\_2},t_{2\_2})$, with $t_{1\_2}=h_1$, $t_{2\_2}=h_2$ (in respect of the fast time t_2) from the column 2 to the column p_2+1 and so on until we arrive in the point $\bar{t}(2,p_2+1)$, with $t_{1\_2}=h_1$, $t_{2\_p2+1}=p_2h_2=T_2$. After that, we integrate one time step h_1 in respect of the slow time t_1 –assigning to $\hat{\boldsymbol{x}}(2,1)$ the value of $\hat{\boldsymbol{x}}(2,p2+1)$ – and then we start again the integration process on the row 3 (in respect of the fast time t_2) from the column 2 to the column p_2+1, and so on until we arrive in the point $\bar{t}(p_1+1,p_2+1)=(t_{1\_p_1+1},t_{2\_p_2+1})$, with $t_{1\_p1+1}=p_1h_1=T_1$ and $t_{2\_p2+1}=p_1h_2p_2=p_1T_2$.

Remark 1. Before passing to the integration for the next grid (each grid having the size $(p_1+1)\times(p_2+1)$), starting from the point $\bar{t}(p_1+2,2)=(t_{1\_p1+2},t_{2\_2})$, with $t_{1\_p1+2}=(p_1+1)h_1$, $t_{2\_2}=p_1T_2+h_2$, we must consider the following boundary conditions:
$\hat{\boldsymbol{x}}(p_1+2,1)=\hat{\boldsymbol{x}}(p_1+1,p_2+1)$, and respectively $\hat{\boldsymbol{x}}(p_1+i,1)=\hat{\boldsymbol{x}}(p_1+i\text{-}1,p_2+1)$, with $i=\overline{3,p_1+1}$ on

the column $t_2 = 0$, and $\hat{\boldsymbol{x}}(p_1+1,j)$, $j = \overline{2, p_2+1}$ on the row $t_1 = T_1$. After that, an integration with the integration step h_1 in respect of the slow time t_1 is performed from the point $\bar{t}(p_1+1, p_2+1)$ to the point $\bar{t}(p_1+2,2)$ (in this point we assign to $\hat{x}(1, p_1+2)$ the value of $\hat{x}(p_2+1, p_1+1)$) (Fig. 1).

Proceeding in this way for the other periods T_1 and T_2 we shall integrate the MPDE on the whole uniform grid of size $(p_2+1)\times(n_1+1)$, arriving in the point $\bar{t}(n_1+1,p_2+1) = (t_{1\_n_1+1}, t_{2\_p_2+1})$, with $t_{1\_n_1+1} = m_1 T_1$, and $t_{2\_p_2+1} = n_1 T_2$. At each time $\bar{t}(i,j)$ we have to solve a system of nonlinear algebraic equations. To this end we can use the Newton-Raphson algorithm or other efficient numerical iteration algorithms.

The discrete resistive circuit equations, associated with the BDF of the first order ($a_0 = 1$ and $a_1 = -1$) when the characteristics of the nonlinear elements are approximated by piecewise-linear continuous curves, at $\bar{t}(i,j)$ (with $t_{1i} = (i-1)h_1$, $t_{2j} = (i-1)T_2 + (j-1)h_2$) (at each integration step h_1 we perform p_2 integrations with size step h_2), and at the $(k+1)^{th}$ iteration of the Newton-Raphson algorithm, corresponding to the state equations (1), have the following form:

$$\frac{1}{h_1}(\boldsymbol{x}_{\_n} - \boldsymbol{x}_{\_o1}) + \frac{1}{h_2}(\boldsymbol{x}_{\_n} - \boldsymbol{x}_{\_o2}) = \boldsymbol{A}\boldsymbol{x}_{\_n} + \boldsymbol{B}\boldsymbol{y}_{\_n} + \\ + \boldsymbol{B}_1\left[\frac{1}{h_1}(\boldsymbol{y}_{\_n} - \boldsymbol{y}_{\_o1}) + \frac{1}{h_2}(\boldsymbol{y}_{\_n} - \boldsymbol{y}_{\_o2})\right], \quad (5)$$

where: $x_{\_n} = x(i,j)$ is the new value of the state vector $\boldsymbol{x}$ at the moment $\bar{t}(i,j)$, $\boldsymbol{x}_{\_o1} = \boldsymbol{x}(i-1,j)$ ($\boldsymbol{x}_{\_o2} = \boldsymbol{x}(i,j-1)$) is the "old" value of the state vector $\boldsymbol{x}$. at the moment $\bar{t}(i-1,j)$ (at the moment $\bar{t}(i,j-1)$), $\boldsymbol{y}_{\_n} = \boldsymbol{y}(i,j)$ is the new value of input vector $\boldsymbol{y}$ at $\bar{t}(i,j)$, $\boldsymbol{y}_{\_o1} = \boldsymbol{y}(i-1,j)$ ($\boldsymbol{y}_{\_o2} = \boldsymbol{y}(i,j-1)$) is the "old" value of the input vector $\boldsymbol{y}$ at the moment $\bar{t}(i-1,j)$ (at the moment $\bar{t}(i,j-1)$). The vectors: $\boldsymbol{y}(i,j)$, $\boldsymbol{y}(i-1,j)$ and $\boldsymbol{y}(i,j-1)$ represent the contributions of the excitation sources (independent current and voltage sources), of the sources corresponding to the approximations of nonlinear resistors and the initial values of the inductor currents and of the capacitor voltages which are determined from the previous time steps $\bar{t}(i,j-1)$ of the slow time t_1, and $\bar{t}(i-1,j)$ of the fast time t_2. The subscripts (i, j), $(i\text{-}1, j)$, $(1,j)$ and $(1,j\text{-}1)$ represent the time moments.

The structure of the equations (5) leads to the elimination of the state variable that appears in the least number of state equations. Elimination procedure is equivalent to substituting the variables involved in the smallest number of equations and removing the equations involving the smallest number of variables (some of them are the variables to be eliminated) in the state equations (5). According to this rule, we select the state equations corresponding to the eliminated state variables and introducing them in the remained state equations, we obtain the state equations in the normal form for the remained state variables. These state equations have as symbols the old values of all state variables and time step size. The remained state equations can easy be integrated to obtain the circuit response. With this approach we obtain important savings in computing time and memory.

3. EXAMPLE

In Fig. 2 is shown the equivalent circuit for the TV video-frequency circuit. The voltage-controlled nonlinear resistor R_{13} is modeled by an equivalent scheme corresponding to the approximation of the *v-i* characteristic by a continuous piecewise linear curve:

U_{13} [V]	-1000.0	0.0	0.1	100.0
I_{13} [mA]	-1.0e-15	0.0	10.0	10000.0

The state vector has the following structure:

$$\boldsymbol{X}=[\text{UC5,UC6,UC7,UC8,UC9,IL22,IL23,IL24,UC2,UC4,UC3}]^t \quad (6)$$

The eliminated state variables are:

$$\textbf{\textit{el\_st\_var s}} = [\text{UC5,IL22,IL23,IL24,UC9,UC4}]^t \quad (7)$$

The remained state equations in partially-symbolic normal form, when we consider as symbols the input vector, the "old" value of state variables and the associated parameters to the nonlinear circuit elements, (the full symbolic form can be obtained, but it is a very large expression) of the circuit in Fig. 2, have the form:

```
Rem_st_eqs:={1.500*UC8_n-.5000*UC8_o1-1.000*UC8_o2 =
 .2859e-1*UC5_o2+.1624e-4*e1+.1429e-1*UC5_o1+
.4639e-3*IL22_o1+.9278e-3*IL22_o2+.4290e-1*UC6_n-
.2893e-1*UC9_o2+.2706e-3*IL23_o2+.1353e-3*IL24_o1+
.2706e-3*IL24_o2-.1624e-4*UC2_n+.2639e-3*UC4_o1+
.5280e-3*UC4_o2+.2593e-4*UC3_n-.4505e-1*UC8_n-
.8078e-5*UC7_n+.1353e-3*IL23_o1-.1446e-1*UC9_o1 ;

 1.500*UC3_n-.5000*UC3_o1-1.000*UC3_o2 =
 -.2131e-1*UC5_o2+.1268e-2*e1-.1066e-1*UC5_o1-
.1138e-1*IL22_o1-.2276e-1*IL22_o2-.3249e-1*UC6_n+
.1245e-1*UC9_o2-.6638e-2*IL23_o2-.3319e-2*IL24_o1-
.6638e-2*IL24_o2-.1268e-2*UC2_n+.4683e-2*UC4_o1+
.9367e-2*UC4_o2-.2303e-2*UC3_n+.1879e-1*UC8_n+
.1981e-3*UC7_n-.3319e-2*IL23_o1+.6220e-2*UC9_o1 ;

1.500*UC6_n-.5000*UC6_o1-1.000*UC6_o2 =
 -.1204e-1*UC5_o2+.1540e-3*e1-.6017e-2*UC5_o1+
.4401e-2*IL22_o1+.8804e-2*IL22_o2-.2003e-1*UC6_n+
.6654e-2*UC9_o2-.2520e-1*IL23_o2-.1261e-1*IL24_o1-
.2520e-1*IL24_o2-.1540e-3*UC2_n+.2505e-2*UC4_o1+
.5011e-2*UC4_o2+.2460e-3*UC3_n+.1006e-1*UC8_n+
.7525e-3*UC7_n-.1261e-1*IL23_o1+.3327e-2*UC9_o1 ;
```

1.500*UC7_n-.5000*UC7_o1-1.000*UC7_o2 =
-.3074e-1*UC7_n+.1960e-1*IL23_o1+.3922e-1*IL23_o2+.1170e-2*UC6_n ;

1.500*UC2_n-.5000*UC2_o1-1.000*UC2_o2 =
.8335e-2*e1-.8335e-2*UC3_n-.8335e-2*UC2_n-.5000/Rdu13*UC2_n-.5000*Ij14} ;

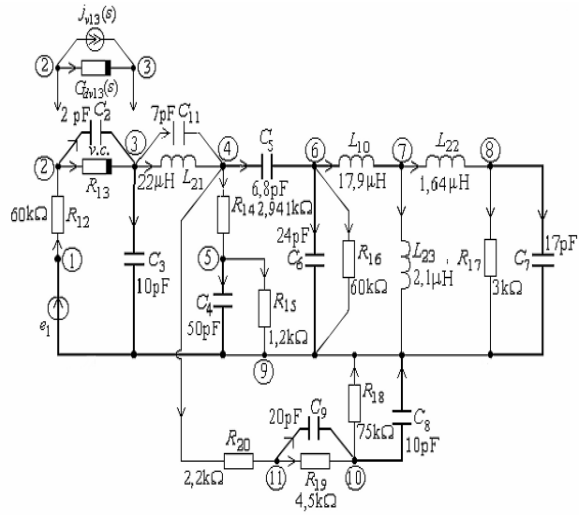

Figure 2. Diagram of the TV video-frequency circuit.

If we assume that the input signal $e_1(t)$ has the following expression:

$$e_1(t) = (1.0 + 0.9\sin(2\pi f_{MA} t))\sin(2\pi f_0)\ V,$$
$$f_{MA} = 4MHz, \quad f_0 = 400MHz$$

The bi-variate excitations have the expressions:

$$\hat{e}_1(t_1, t_2) = (1.0 + 0.9\sin(2\pi f_{MA} t_1))\sin(2\pi f_0 t_2)\ V,$$
$$f_{MA} = 4MHz, \quad f_0 = 400MHz$$

and was plotted in Fig. 3.

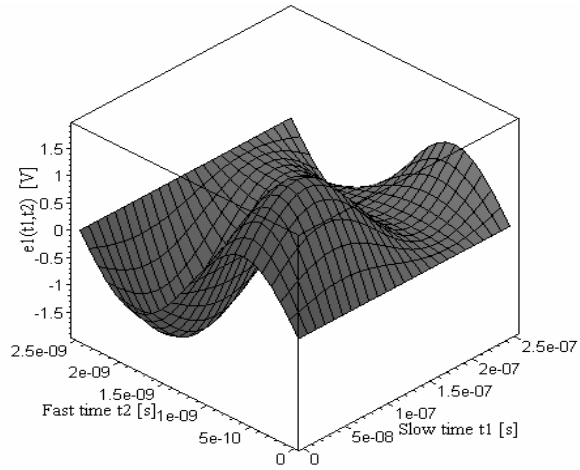

Figure 3. The bi-variate excitation $e_1(t_1,t_2)$.

Using the method presented in Section 2 the variations of the capacitor voltages v_{C2}, v_{C8} and the inductor current i_{L21}, in respect to the time, are shown in Figures 4, 6, and 8, respectively, in a representation with two-time variables, and in Figures 5, 7, and 9, respectively, in a one-time variable representation.

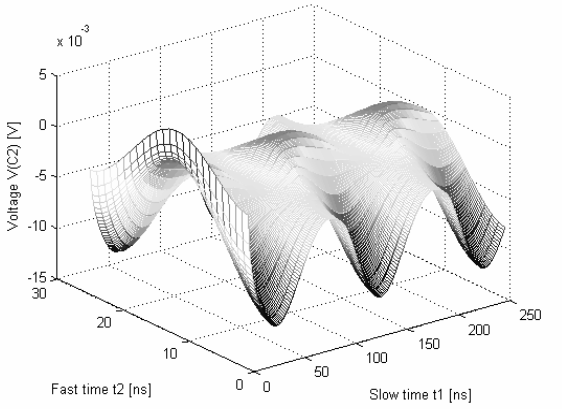

Figure 4. Two-time variation of the output voltage vC2

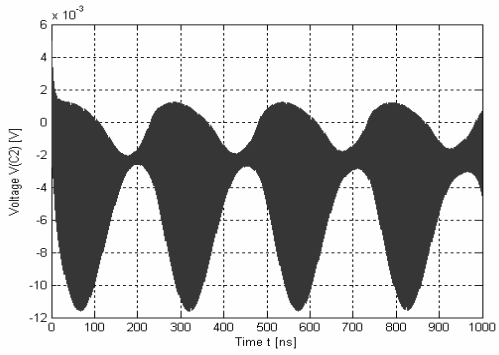

Figure 5. One-time variation of the output voltage vC2.

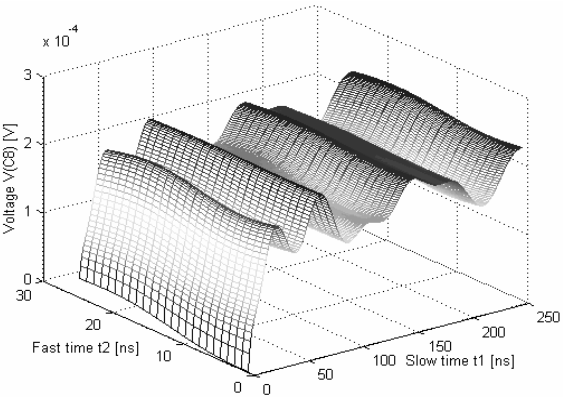

Figure 6. Two-time variation of the output voltage vC8.

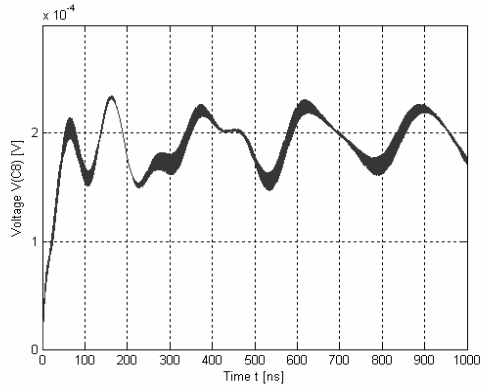

Figure 7. One-time variation of the output voltage vC8.

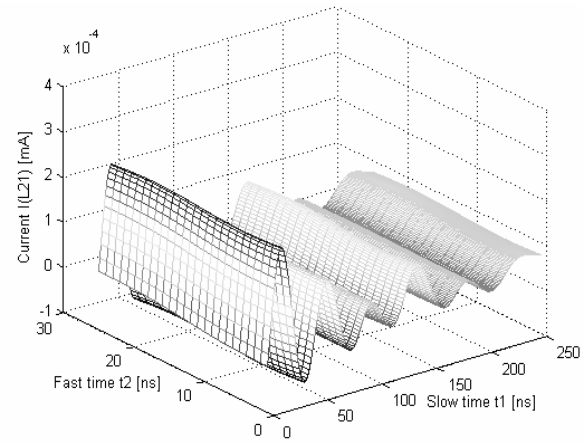

Figure 8. Two-time variation of the output voltageiL21.

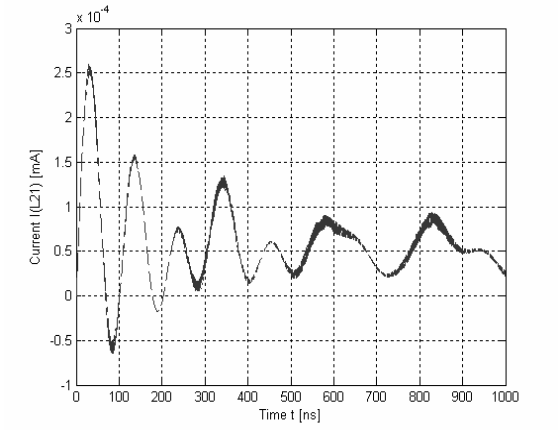

Figure 9. One-time variation of the output voltage iL21.

4. CONCLUSIONS

An efficient numerical approach for analyzing strongly nonlinear multirate circuits has been presented. The procedure uses multiple time variables to describe multirate behaviour, leading to a PDE called MPDE. Applying appropriate BCs to this MPDE, and using the state equations lead to quasi-periodic and envelope-modulated solutions. By using the backward differential formula of high order, the efficiency is achieved without compromising accuracy. Presenting the results in three-dimensional form is useful for visualizing waveforms with widely separated time scales (as in the case of RF-IC). The new technique can solve a variety of circuits with a mixture of strong and weak nonlinearities that are hard to simulate otherway.

Acknowledgments

This research is financed from CNCSIS grant – C38.

References

[1] J. Roychowdhury, Analyzing Circuits with Widely Separated Time Scales Using Numerical PDE Methods, IEEE Trans. on CAS – I, **48**, 5, pp. 578-594 (2001).

[2] Fl. Constantinescu, Miruna Nitescu, A new multi-rate method for analysis of RF-IC circuits, Proc. of the International Symposium on Signals, Circuits and Systems, SCS'03, Iasi, Romania, July, 10-11, pp. 91-94 (2001).

[3] H. G. Brachtendorf, G. Welsch, R. L. Laur, A novel time-frequency method for the simulation of the steady state of circuits driven by multi-tone signals, Proc. on ISCAS, June 9-12, Hong Kong, pp.1508-1511(1997).

[4] C.W. Ho, A. E. Ruehli, P. A. Brennan, The modified nodal approach to network analysis, IEEE, Trans., CAS, **22**, 5, pp. 504-509 (1975).

[5] A. E. Schwarz, Computer-aided design of microelectronic circuits and systems, Academic Press, London, 1987.

[6] L. O. Chua, and P. M. Lin, Computer-Aided Analysis of Electronic Circuits: Algorithms and Computational Techniques, Englewood Cliffs, NJ: Prentice-Hall, 1975.

[7] A. Ushida, L. O. Chua, Frequency-domain analysis of nonlinear circuits driven by multi-tone signals, IEEE Trans. on Circuits and Systems , **31**, 9, pp. 766-779 (1984).

[8] M. Iordache, M. Perpelea, Modified nodal analysis for large-scale piecewise-linear nonlinear electric circuits, Rev., Roum., Sci., Techn., - Électrotechn. et Énerg., **37**, 4, pp. 487-496 (1992).

[9] M. Iordache, Lucia Dumitriu, L. Mandache, Time-Domain Modified Nodal Analysis for Large-Scale Analog Circuits, Revue Roum. Sci. Techn. - Électrotechn. et Énerg., **48**, 2-3, pp. 257-268 (2003).

[10] M. Iordache**,** Lucia Dumitriu**,** Efficient Decomposition Techniques for Symbolic Analysis

of Large – Scale Analog Circuits by State Variable Method, Analog Circuits and Signal Processing, Kluwer**, 40**, 3, Kluwer Academic Publishers, pp.235-253 (2004).

[11] Angela M. Hodge, R. W. Newcomb, Semistate Theory and Analog VLSI Design, IEEE Circuit and Systems Magazine, **2,** 2, pp.30-49 (2002).

[12] L. Mandache, M. Iordache, Lucia Dumitriu, Time-Domain Modified Nodal Analysis for Analog Circuits, Proceeding of 7th International Workshop on Symbolic Methods and Applications in Circuit Design, SMACD 2002, October 10-11, Sinaia, Romania, pp. 71-76 (2002).

[13] R. Achar, M.S. Nakhla, Simulation of High-Speed Interconnects, Proceeding of the IEEE, Vol. 89, No. 5, May 2000, pp. 693-728.